

Boron carbide structure by Raman spectroscopy

D. R. Tallant, T. L. Aselage, A. N. Campbell, and D. Emin

Sandia National Laboratories, Albuquerque, New Mexico 87185

(Received 27 March 1989)

We have obtained and analyzed Raman spectra of single-crystal, hot-pressed, and chemical-vapor-deposited boron carbide materials over their single-phase region (from ~ 9 to ~ 20 at. % carbon). These spectra provide insight into the substitutional disorder that characterizes these structurally ordered solids. In particular, although icosahedra and chain structures occupy regular lattice positions, there is local substitutional disorder resulting from the occupancy of certain sites within the icosahedra and chains by either boron or carbon atoms. Comparison of boron carbide Raman spectra with the Raman spectra of α -rhombohedral boron, boron phosphide, and boron arsenide has confirmed the following structural model derived from theoretical considerations and electrical and thermal transport data. The boron carbide composition with nearly 20 at. % carbon is composed of $B_{11}C$ icosahedra linked by carbon-boron-carbon chains. As the carbon content is reduced toward approximately 13 at. %, carbon-boron-carbon chains are progressively replaced by carbon-boron-boron chains. Further reduction in the carbon content results in the replacement of $B_{11}C$ icosahedra with B_{12} icosahedra.

INTRODUCTION

Icosahedral boron-rich solids are refractory solids with melting temperatures up to 2400 °C. Of these solids, the boron carbides are degenerate semiconductors with near-term applications as high-temperature thermoelectric materials.¹ The wide-band-gap (> 3.3 eV) insulating icosahedral boron-rich pnictides, $B_{12}P_2$ and $B_{12}As_2$, when suitably doped, have potential applications as high-temperature semiconductors.²

Structure

The icosahedral boron-rich solids are based on the structure of α -rhombohedral boron.³ As illustrated in Fig. 1(a) α -rhombohedral boron is composed of boron icosahedra (12-atom clusters) located at the corners of a rhombohedral unit cell.⁴ Three-center bonds [the shaded triangles in Fig. 1(a)] join icosahedra along the threefold

axis of the unit cell. In the icosahedral boron-rich pnictides [Fig. 1(b)], a chain composed of two phosphorus or two arsenic atoms joins the icosahedra. In the boron carbides [Fig. 1(c)], a three-atom chain joins the icosahedra. Both types of chain structures reside along the longest diagonal of the unit cell. All three types of icosahedral boron-rich solids have strong structural similarities in their icosahedral skeletons. In each icosahedron, six atoms bond directly to other icosahedra via strong two-center bonds along the cell edges. These six atoms reside in two "polar" triangles on opposite ends of the icosahedron. The remaining six icosahedral atoms occupy "equatorial" sites. The atoms in the equatorial sites either bond directly to other icosahedra through three-center bonds, as in α -rhombohedral boron, or bond to chain structures, as in the boron pnictides and carbides.

The boron carbides exist as a single-phase material from about 9 at. % carbon to about 20 at. % carbon.⁵ A model based on early x-ray diffraction data⁶ and more recent ^{13}C NMR data⁷ proposes that the 20 at. % carbon composition is made up of B_{12} icosahedra and carbon-carbon-carbon (CCC) chains. Other models⁸⁻¹⁰ for the 20 at. % carbon composition specify $B_{11}C$ icosahedra and carbon-boron-carbon (CBC) chains. These models are supported by later x-ray diffraction³ as well as ^{11}B NMR data.^{4,11} Among those who favor the $B_{11}C$ icosahedra-CBC chain model for the 20 at. % composition, there is disagreement on the structural changes that occur in boron carbides as the carbon content is decreased toward 13 %. Some workers,^{10,12,13} citing x-ray diffraction data, propose that carbon atoms are removed from the icosahedra to form B_{12} icosahedra. Other workers,^{8,9} citing electrical and thermal transport measurements and supported by a theoretical analysis of the free energies of boron carbide structures,¹⁴ propose that, as the carbon concentration is reduced, boron atoms substitute preferentially

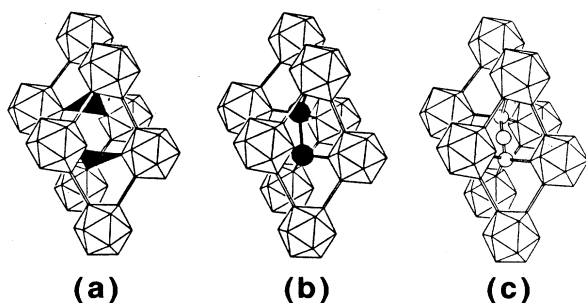


FIG. 1. Structure of icosahedral boron-rich materials. (a) α -rhombohedral boron, (b) boron phosphide or boron arsenide, (c) boron carbide.

for carbon within the three-atom intericosahedral chains.

Electronic transport

The electrical conductivity of boron carbides measured between 77 and 1200 K is consistent with the hopping of a large ($\approx 10^{21} \text{ cm}^{-3}$) composition-dependent, but temperature-independent, density of small bipolarons between $B_{11}C$ icosahedra.⁸ This view is supported by the presence of low, thermally activated Hall mobilities in these materials.⁸ Measurements of their thermoelectric (Seebeck) coefficients between 10 and 20 at. % carbon always indicate *p*-type hopping motion.⁸ Furthermore, the Seebeck coefficient manifests a large temperature-dependent contribution that is consistent with hopping between inequivalent sites.¹⁵ The persistence of *p*-type electrical transport throughout this composition regime is consistent with hopping between $B_{11}C$ icosahedra but not between B_{12} icosahedra. Furthermore, the disorder inherent in carbon containing (but not B_{12}) icosahedra due to placement of carbon atoms in structurally inequivalent locations is consistent with the temperature dependence of the thermoelectric coefficient.

Magnetic susceptibility and electron-spin resonance (ESR) measurements indicate a temperature-independent density of spins that is much smaller ($\approx 10^{19} \text{ cm}^{-3}$) than the density of charge carriers.¹⁶ Furthermore, the ESR of the small number of spins that are observed is associated with a "defect" that occurs when a carbon atom occupies the central position of a three-atom chain.^{17,18} These results imply that the charge carriers are spinless.

The presence of spinless charge carriers can be explained by the pairing of electrons to form singlet bipolarons. While the occurrence of small bipolarons is rare in solids, boron-rich icosahedral solids have properties that favor their formation.¹⁹ A bipolaron is formed when a pair of electrons is added to a boron-rich icosahedron, completing the filling of its internal bonding orbitals and contracting the icosahedron.¹⁹ Since the electronic density of an icosahedron is confined to its surface,³ the Coulombic repulsion, which usually precludes the pairing of charge carriers, is relatively small. A B_{12} icosahedron requires two additional electrons to fill its internal bonding orbitals and forms doubly charged $(B_{12})^{2-}$. A $B_{11}C$ icosahedron requires one additional electron to fill its internal bonding orbitals. The resulting icosahedron $(B_{11}C)^-$ has a single, negative charge. The lower Coulomb energy of the $(B_{11}C)^-$ icosahedron favors its formation. The bonding orbitals of a $B_{10}C_2$ icosahedron would be filled without the addition of electrons and would not be a site for bipolaron formation.

Thus, the electronic transport in boron carbides from 10 to 20 at. % carbon is thought to proceed by the hopping of pairs of electrons between $B_{11}C$ icosahedra: $(B_{11}C)^- + (B_{11}C)^+ \rightarrow (B_{11}C)^+ + (B_{11}C)^-$. The conduction is *p* type over this composition region because the intericosahedral chains donate electrons to the $B_{11}C$ icosahedra, so that more than half of the $B_{11}C$ sites are negatively charged.¹⁹ If, as suggested by the electronic transport data, $B_{11}C$ icosahedra persist even at a carbon

content of 10 at. %, then it can be inferred that boron replaces carbon preferentially within the intericosahedral chains (rather than within the icosahedra) as the carbon concentration is reduced from 20 at. %.

Thermal transport

Boron carbides also exhibit unusual thermal transport properties. Composed of light atoms and displaying exceptional hardness, they should be good thermal conductors. Thermal conductivity measurements, however, suggest a more complex behavior. At a nominal composition of 20 at. % carbon, the thermal conductivity falls with temperature in the manner characteristic of crystals (Fig. 2). However, the thermal transport of boron carbides containing significantly less than 20 at. % carbon is relatively low and temperature independent,²⁰ a behavior more characteristic of amorphous materials. These differences in thermal transport can be explained if it is assumed that the thermal conductivity is dominated by the transfer of vibrational energy through the intericosahedral chains rather than through the "softer" icosahedra.²¹ Then, the coherent transport of thermal energy is disrupted by disorder in the intericosahedral chains as the CBC chains are inhomogeneously replaced with CBB chains. With much softer boron-boron bonds in the CBB chains than the carbon-boron bonds comprising the CBC chains,²¹ the effect of this disorder can be dramatic. Thus, converting CBC chains to CBB chains can result in a transition from crystal-like to glasslike thermal transport.

Raman spectroscopy

From free-energy calculations and the electronic transport, thermal transport, and magnetic measurements discussed above, it can be inferred that boron carbides con-

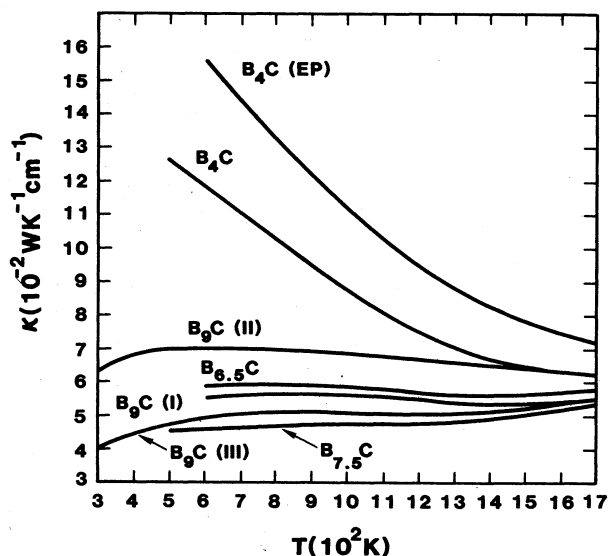


FIG. 2. The thermal conductivity (κ) of boron carbides as a function of temperature (T); from Ref. 20.

taining nearly 20 at. % carbon are composed of $B_{11}C$ icosahedra linked by CBC chains and that lower carbon compositions are formed by replacing CBC chains with CBB chains. However, none of these techniques provide, directly, the structural information needed to distinguish this model from the others that have been proposed. Raman spectroscopy, on the other hand, provides information on the vibrational modes and, therefore, the atomic structure of both amorphous and crystalline materials.

A Raman spectroscopic study has been carried out on bulk boron carbides and on films prepared by chemical-vapor deposition (CVD), whose compositions varied over the entire single-phase region. Raman spectra were also obtained of α -rhombohedral boron and the icosahedral boron pnictides. The Raman spectrum of the nearly 20 at. % carbon composition is consistent with $B_{11}C$ icosahedra and CBC chains. Spectra of compositions containing 20 to 13 at. % carbon are consistent with the progressive loss of carbon from CBC chains to form CBB chains. Spectra of compositions containing 13 to 8 at. % carbon are consistent with the progressive conversion of $B_{11}C$ icosahedra to B_{12} icosahedra. The results of this study provide direct evidence in support of the boron carbide structural model inferred from electronic and thermal transport measurements.

EXPERIMENTAL

Polycrystalline boron carbide samples were prepared by hot pressing or by chemical vapor deposition. Hot-pressed isotopically enriched (98.5%) ^{11}B samples were prepared from either boron carbide powders or from mixtures of boron with graphite. The latter mixtures were pretreated by dry shaking for several hours. The powders were pressed in graphite dies with high purity boron nitride liners at 2150 to 2200 °C and at uniaxial pressures between 5500 and 6000 psi. Samples typically achieved densities greater than 99% of theoretical with these pressing conditions. Prior to Raman analysis, a portion of the surface of each sample was ground and polished to remove any contamination from the die. The compositions quoted for the hot-pressed samples are based on the ratios of boron to carbon in the starting materials.

Polycrystalline boron carbide deposits up to 0.2 mm thick were also produced by CVD on inductively heated graphite substrates by decomposition of electronic-grade BCl_3 and CCl_4 in the presence of excess H_2 . The CCl_4 was vaporized in a bubbler with Ar as the carrier gas. The details of the experimental apparatus were previously reported.²² The compositions of the deposits were determined by Auger spectroscopy. Phase identification was accomplished by selected area electron diffraction and by x-ray diffraction.

Single crystals of α -rhombohedral boron, icosahedral boron arsenide ($B_{12}As_2$), and boron carbide were prepared by recrystallization from solution. Isothermal saturation of molten palladium-boron alloys, using vapor sources of boron and arsenic, was used to grow α -rhombohedral boron and boron arsenide crystals. The α -rhombohedral boron formed small (0.1–0.5 mm),

translucent red crystals. Thin specimens of boron arsenide crystals were nearly transparent. Boron carbide crystals were prepared by dissolving boron carbide into copper or palladium at 1750 to 1800 °C, followed by slow cooling at 5–20 °C/h.²³ The resulting boron carbide crystals were up to 3 mm in size, displaying shiny black facets. The icosahedral boron phosphide ($B_{12}P_2$) sample was obtained in powder form from Noah Chemical Company.

Raman spectra were obtained using a computer-controlled, scanning, double monochromator equipped with holographic gratings and a photon-counting photomultiplier tube.²⁴ The single crystal samples of α -rhombohedral boron and boron arsenide were illuminated using a microscope accessory. The remaining samples were illuminated with the laser beam focused to a 0.1×2 mm line. Unless otherwise noted, the 514.5-nm argon laser line was used for excitation. Background features (Rayleigh scatter, fluorescence) were removed by empirical fitting procedures. The vertical (count) axes of the spectra within a given figure have been scaled so as to normalize one of the more intense Raman bands in each spectrum.

RESULTS AND DISCUSSION

In our analysis of the Raman spectra of the boron carbides, we will make two types of comparisons. First, the spectrum of the 20 at. % carbon composition will be compared with spectra of other icosahedral boron-rich materials in order to assign the observed Raman bands to vibrations of either icosahedral or chain structures and to determine the general level of order and/or disorder in each type of structure. Second, the Raman spectra of boron carbides with compositions ranging from ~20 to ~8 at. % carbon will be compared to each other. The goal of the second comparison is to identify changes in the icosahedral and/or chain structures as boron atoms replace carbon atoms in the boron carbide lattice.

Other icosahedral borides

Figure 3 displays the Raman spectra of (from top to bottom) a single crystal of boron arsenide, boron phosphide powder, a single crystal of α -rhombohedral boron, and a single crystal of boron carbide. The spectrum of α -rhombohedral boron is composed of narrow bands consistent with a regular, crystalline structure. Note that the band complex at 1100 to 1200 cm^{-1} , which has been associated with the B_{12} icosahedral breathing mode,²⁵ represents the overlap of a number of narrow bands. This becomes more apparent when the orientation of the crystal is changed. The Raman band in the 100 to 200 cm^{-1} region of the α -rhombohedral boron spectrum is believed to be due to a librational mode.^{26,27}

The feature of 527 cm^{-1} in the α -rhombohedral boron spectrum has an extremely small bandwidth (0.8 cm^{-1} full width at half maximum by our measurements), and it has been considered spurious by other workers.^{26,28} However, it has been observed using both different Raman instruments^{26–28} and different laser excitation fre-

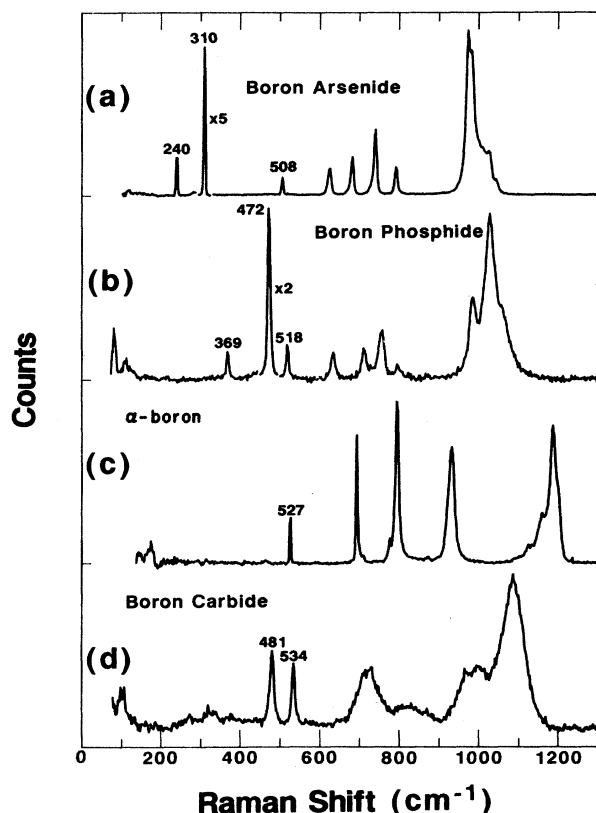


FIG. 3. Background-corrected Raman spectra of icosahedral boron-rich materials with normal isotopic ratios. (a) Single-crystal boron arsenide, (b) boron phosphide powder, (c) single-crystal α -rhombohedral boron, (d) single-crystal boron carbide (20 at. % carbon).

quencies (our work, see also Ref. 27). We have observed the 527 cm^{-1} band in the anti-Stokes Raman region, and the Stokes to anti-Stokes intensity ratios indicate that the populations of the states contributing to this band have a Boltzmann temperature dependence. Therefore, this feature is neither an instrumental artifact nor a nonlasing emission line from the laser plasma. Our studies on an oriented α -rhombohedral boron crystal indicate that the 527 cm^{-1} band is not due to a local vibrational mode, since its symmetry species is neither A_{1g} nor E_g (the only Raman-active symmetries for the D_{3d} point group²⁸). Investigations to determine the source of this feature are continuing.

The remaining features in the spectrum of α -rhombohedral boron range in frequency from 690 to 1200 cm^{-1} . These features have A_{1g} or E_g symmetries and are, therefore, consistent with Raman bands arising from intricosahedral or intericosahedral boron-boron bonds. The assignments of the features from 690 to 1200 cm^{-1} to vibrational modes of the icosahedra can be made unambiguously since α -rhombohedral boron has no other (e.g., chain) structures which could contribute to the observed Raman bands.

The bands in the Raman spectra of the two icosahedral

boron pnictides [Figs. 3(a) and 3(b)] have the small bandwidths characteristic of highly ordered materials. The pattern of pnictide band frequencies in the upper half of the frequency region shown is similar to that of α -rhombohedral boron but appears to be shifted to lower frequency. This shift to lower frequency is consistent with significantly larger intericosahedral and polar triangle bond distances in the pnictides as compared to α -rhombohedral boron.³ We, therefore, assign the bands between 600 and 1100 cm^{-1} in the boron pnictide spectra to intricosahedral or intericosahedral vibrational modes.

The spectra of the boron pnictides also show a number of features in the 200 to 600 cm^{-1} region which are related to structural features present in the boron pnictides but not present in α -rhombohedral boron, i.e., the As-As and P-P chains. The assignment of these bands to chain modes is supported by theoretical and experimental evidence. Normal coordinate calculations²⁵ show that the 310 cm^{-1} band in the boron arsenide spectrum and the 472 cm^{-1} band in the boron phosphide spectrum are very close to calculated values for As-As and P-P stretching modes. Furthermore, the relative intensity of the 310 cm^{-1} band in the boron arsenide spectrum is highly sensitive to the crystal orientation, a characteristic expected of axially oriented chain modes but not axially symmetric icosahedral modes. The 240 cm^{-1} band in the boron arsenide spectrum and the 369 cm^{-1} band in the boron phosphide spectrum may be due to icosahedron-chain (B-As or B-P) modes.

Normal coordinate calculations²⁵ provide reasonable frequency matches for all the bands in the boron arsenide and the boron phosphide spectra except the 508 cm^{-1} band (boron arsenide) and the 518 cm^{-1} band (boron phosphide). These bands may have an origin similar to that of the 527 cm^{-1} band in the α -rhombohedral boron spectrum. Polarization analyses of an oriented boron arsenide crystal indicate that the 508 cm^{-1} band is likewise not consistent with the D_{3d} symmetry expected for boron arsenide. Further, the 508 cm^{-1} band has approximately the same bandwidth as the 527 cm^{-1} band in the spectrum of α -rhombohedral boron.

From the analysis of the α -rhombohedral boron and the boron pnictide spectra, we can draw some general conclusions that will guide the analysis of the boron carbide spectrum. First, the intricosahedral and intericosahedral modes are expected both below 200 cm^{-1} (for librational modes) and above 600 cm^{-1} . For regular B_{12} icosahedra (as present in α -rhombohedral boron and the boron pnictides) the Raman bands representing these modes have the small bandwidths characteristic of highly ordered materials. Apart from the unexplained, exceptionally narrow features near 500 cm^{-1} , any Raman bands occurring between 200 and 600 cm^{-1} can be assigned to chain structures linking icosahedra. These Raman bands will have small bandwidths if they are due to regular chain structures.

B_4C single crystal

Figure 3(d) displays the Raman spectrum of a single crystal of boron carbide that was crystallized from a

copper melt containing boron and carbon in an atomic ratio of 4:1. The lattice constants of such boron carbide single crystals are consistent with a composition containing 20 at. % carbon. This spectrum is seen to be a combination of narrow and broad bands. The broad bands are typically more characteristic of an amorphous, or, at least, a partially disordered structure. The frequency range of the prominent broad bands lies within the frequency range of the icosahedral bands of α -rhombohedral boron (above 600 cm^{-1}), which leads us to assign these bands to icosahedral modes of boron carbide. The presence of a carbon atom within each boron carbide icosahedron is consistent with the relatively large bandwidths of the icosahedral modes. A single carbon atom can reside on one of the six polar or six equatorial sites of the icosahedron, introducing a form of substitutional disorder. In an isolated icosahedron all the polar and all the equatorial sites would be geometrically equivalent. However, the deformation present on one icosahedron due to the presence of a carbon atom is experienced as an altered environment by neighboring icosahedra due to intericosahedral bonding. The greater stiffness of intericosahedral bonds as compared to intraicosahedral bonds^{19,29} accentuates this effect. Thus, the $B_{11}C$ icosahedra experience anisotropy in their immediate environment due to a distribution of carbon atoms among the icosahedral sites. The result of this anisotropy is the observed broadening of the icosahedral vibrational bands of the boron carbides.

Since the two prominent, narrow bands at 481 and 534 cm^{-1} in the single crystal boron carbide spectrum [Fig. 3(d)] are outside the frequency ranges associated with icosahedral modes, we assign them to chain structures linking $B_{11}C$ icosahedra. These two bands vary significantly in their relative intensities as the boron carbide crystal is rotated, as would be expected for an axially oriented chain structure. The intensities of the broad bands due to icosahedral modes are relatively unaffected by crystal rotation. The 534 cm^{-1} band is close in frequency to the 527 cm^{-1} band in the α -rhombohedral boron, but its bandwidth is larger by a factor of 7, and it changes in intensity along with the 481 cm^{-1} band as the carbon content is varied. The 534-cm^{-1} boron carbide band is, therefore, probably not of the same origin as the 527-cm^{-1} α -rhombohedral boron band. The small width of these bands suggests that the chain structure is well ordered. The CBC chains bond through the terminal carbon atoms preferentially to equatorial boron sites on the icosahedra^{3,30} (see Fig. 4). Thus, most CBC chains have the same chain-icosahedron bonding, and all have orientational symmetry. The resulting well-ordered environment is consistent with the narrow width of the Raman bands assigned to chain modes. The preference of CBC chains to bond to boron atoms tends to limit the icosahedral carbon atom to polar sites. The resulting situation is similar to that in $B_{10}C_2$ icosahedra in carboranes ($B_{10}C_2H_{12}$), where the more stable isomers are those with the greatest separation of carbon atoms.³¹

Thus, the Raman spectra for this boron carbide composition (~ 20 at. % carbon) are consistent with the structural model inferred from the transport data. Using

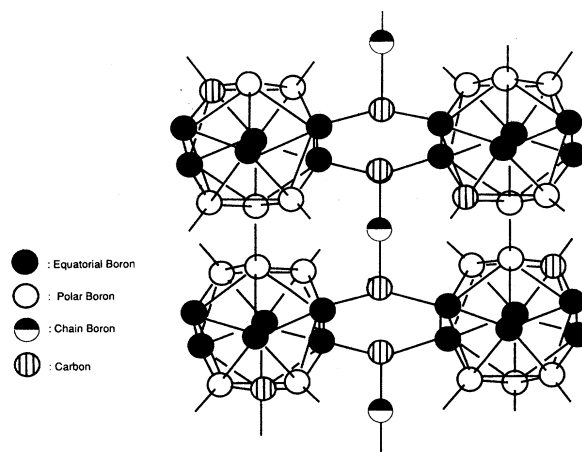


FIG. 4. Structure of a boron carbide containing 20 at. % carbon, showing CBC chains and $B_{11}C$ icosahedra with the carbon atom in polar sites.

this model composition as a reference, we will analyze Raman spectra from samples with different boron to carbon ratios and deduce structural changes as a function of composition.

Effect of varying carbon content

Figure 5 shows the effect of a decrease in carbon composition on the Raman spectra of a series of isotopically enriched (^{11}B) hot-pressed boron carbide samples, while Fig. 6 shows the spectra of two CVD-prepared samples with normal boron isotopic ratios and low-carbon contents. The 200 to 600 cm^{-1} region, which we have associated with the vibrations of chain structures, is affected most strongly by the variation in carbon content. The two narrow bands near 500 cm^{-1} , which we have assigned to vibrations of CBC chains, decrease steadily in intensity with a reduction in carbon content [Figs. 5(a)–5(c)] and have nearly disappeared at 13 at. % carbon [Figs. 5(d) and 6(a)]. Broad bands near 400 cm^{-1} appear and increase in intensity as the carbon content decreases. Two broad bands near 300 cm^{-1} , apparent in the spectra of the 20 and 18 at. % carbon compositions [Figs. 5(a) and 5(b)], also decrease in intensity with carbon content. The bands near 300 cm^{-1} are not as prominent in the spectrum of single crystal boron carbide [Fig. 3(a)]. They may be related to chain-icosahedral linkages. The Raman bands in the 600 to 1200 cm^{-1} region, which are associated with icosahedral modes, are relatively unaffected by changes in carbon content. Nonetheless, the band complex at 900 to 1100 cm^{-1} broadens slightly (or develops more prominent shoulders) as the carbon content decreases to 13 at. %, and then narrows slightly as the carbon content decreases from 13 at. %. The narrowing of this band complex is more apparent in the spectra of the CVD-prepared samples, Fig. 6.

The observed changes in the spectra of Figs. 5 and 6 with carbon content are consistent with the model for carbon replacement inferred from the transport data. In

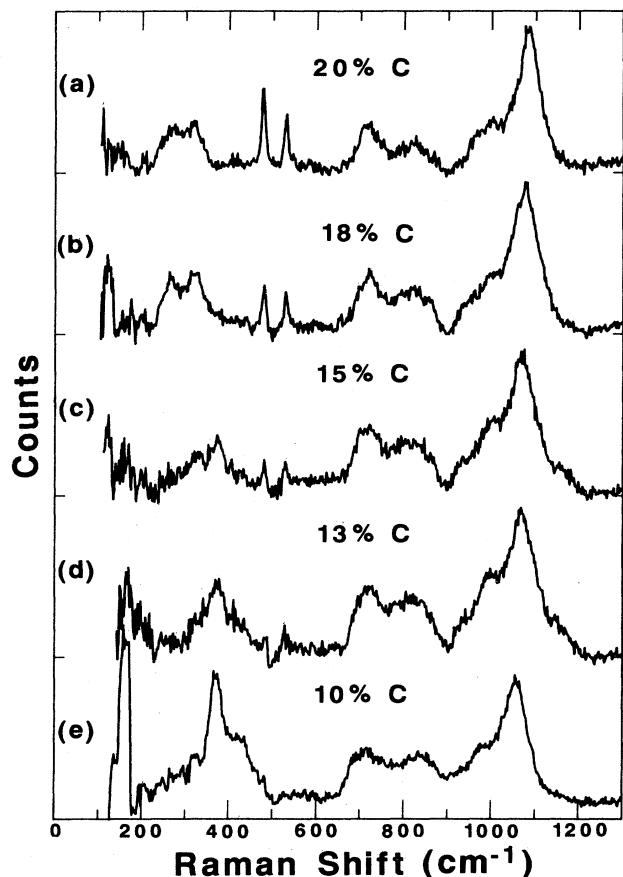


FIG. 5. Background-corrected Raman spectra of hot-pressed, isotopically enriched (^{11}B) boron carbides. (a) 20 at. % carbon, (b) 18 at. % carbon, (c) 15 at. % carbon, (d) 13 at. % carbon, (e) 10 at. % carbon.

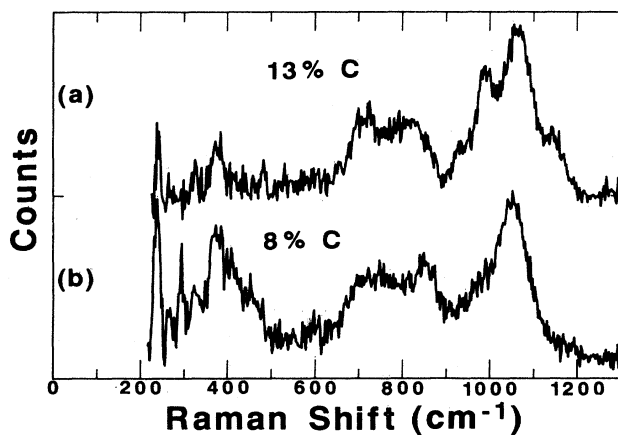


FIG. 6. Background-corrected Raman spectra of chemical-vapor-deposited boron carbides with normal isotopic ratios. (a) 13 at. % carbon, (b) 8 at. % carbon (contains minor amount of a tetragonal boron carbide phase, $\sim\text{B}_{25}\text{C}$).

all these spectra, which span the single-phase region of the boron carbides, the icosahedral bands (600 to 1200 cm^{-1}) are broad compared to the icosahedral bands in the spectra of α -rhombohedral boron and the boron pnictides. The persistence of these broad icosahedral bands suggests that there are a large number of B_{11}C icosahedra present even at the lowest carbon compositions in the single-phase region. Thus, the Raman spectra are not consistent with a model that predicts a highly ordered phase (B_{12} icosahedra and CBC chains) for the 13 at. % carbon composition.

The decrease in intensity of the narrow bands near 500 cm^{-1} and the appearance of broad bands near 400 cm^{-1} corresponds to the replacement of CBC chains with CBB chains. For the same type of vibrational modes, the less stiff CBB chains²¹ will have a lower vibrational frequency than the CBC chains they replace. The vibrational modes of the CBB chains will also yield broader Raman bands than the modes of the CBC chains. As noted previously, CBC chains have orientational symmetry and bond preferentially to boron sites in the icosahedral (Fig. 4). However, the CBB chains have orientational asymmetry, and the boron end of the CBB chain can bond to either icosahedral boron or carbon in an equatorial site. These bonding arrangements are illustrated in Fig. 7, which depicts the structure of a boron carbide whose composition is between 20 and 13 at. % carbon. Both the orientational asymmetry and the variability in chain-icosahedral bonding of the CBB chains will appear as a "disordering" of the local environment with a resultant broadening of the Raman bands due to the chain structures. If boron atoms substitute for carbon atoms only in CBC chains and not in the B_{11}C icosahedra, then the CBC chains will be completely depleted when the carbon content reaches approximately 13 at. % (a boron to carbon ratio of 13:2). In the spectra of both hot-pressed and CVD boron carbide with 13 at. % carbon [Figs. 5(d) and 6(a)], the bands near 500 cm^{-1} associated with CBC

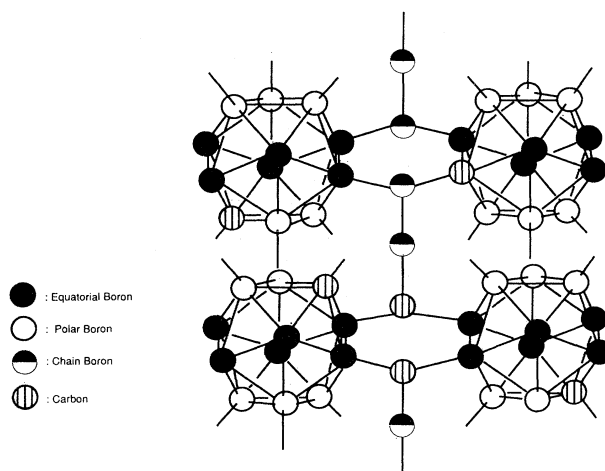


FIG. 7. Structure of a boron carbide containing between 20 and 13 at. % carbon, showing CBB chains and B_{11}C icosahedra with the carbon atom in both polar and equatorial sites.

chains have nearly disappeared.

An additional consequence of the replacement of CBC chains with CBB chains is an increase in the number of icosahedra with carbon atoms in equatorial (chain-bonding) sites, as discussed above. The net result is an increase in substitutional disorder in the icosahedra, since the carbon atoms distribute not only among polar sites but also more freely among equatorial sites. A slight broadening of the Raman bands associated with the icosahedral vibrational modes may be expected from such increased disordering of the icosahedra. The Raman band complex associated with the icosahedral breathing mode (900 to 1100 cm^{-1}) shows a slight broadening as the carbon content is reduced from 20 to 13 at. %.

According to thermodynamic calculations,¹⁴ reductions in carbon content below 13 at. % are accompanied by removal of carbon from B_{11}C icosahedra to form B_{12} icosahedra. The result of the presence of an increasing fraction of ordered B_{12} icosahedra, even with the persistence of orientationally disordered CBB chains, should be a decrease in the width of the Raman band associated with the icosahedral breathing mode. In the spectra of the CVD samples (Fig. 6), the central portion of the icosahedral breathing mode, at $\sim 1060 \text{ cm}^{-1}$, becomes more prominent compared to its shoulders as the carbon content decreases from 13 to 8 at. %. The increased prominence of the central portion of the icosahedral breathing mode is interpreted as reflecting an increased fraction of B_{12} icosahedra. Note that there is not a concomitant shift in the icosahedral breathing mode frequency towards that observed for B_{12} icosahedra in α -rhombohedral boron [Fig. 3(c)]. In the icosahedral boron-rich solids, the intericosahedral and intraicosahedral atomic distances tend to adjust to the structural environment provided by the chains. Therefore, the intericosahedral and intraicosahedral atomic distances of a B_{12} icosahedron in a boron carbide environment are expected to be more similar to that of a B_{11}C icosahedron in boron carbide than to a B_{12} icosahedron in α -rhombohedral boron. Since the frequency of the icosahedral breathing mode is strongly affected by the intericosahedral atomic distances,²⁷ a similarity in the

icosahedral breathing mode frequencies of B_{12} and B_{11}C icosahedra in boron carbides is not unexpected.

SUMMARY

X-ray studies³ have shown that boron carbides consist of an ordered arrangement of icosahedra and intericosahedral chains. The x-ray results also indicate that some of the carbon atoms occupy polar sites on icosahedra composed primarily of boron atoms, while other carbon atoms reside in the chains. These Raman studies establish that the distribution of carbon and boron atoms among inequivalent sites within the icosahedra and chains leads to a form of local, substitutional disorder. The Raman spectra are consistent with a boron carbide structure made up of B_{11}C icosahedra and CBC chains when the carbon content is ~ 20 at. %. The B_{11}C icosahedra appear disordered, but the CBC chains, which most strongly affect the thermal-transport properties, appear regular. A decrease in the carbon content results in replacement of CBC chains with CBB chains until approximately 13 at. % carbon is present. At 13 at. % carbon both the icosahedra and the chains appear disordered. Further reduction in the carbon content results in the replacement of B_{11}C icosahedra with B_{12} icosahedra. This model for the structure of boron carbide over its single-phase region is completely consistent with thermodynamic calculations, with electrical transport measurements, and with the transition from crystalline to glass-like thermal transport with decreasing carbon content.

ACKNOWLEDGMENTS

This work, performed at Sandia National Laboratories, was supported by the U.S. Department of Energy under Contract No. DE-AC04-76-DP00789. The authors thank B. Morosin for orienting the single-crystal samples, A. W. Mullendore for providing the CVD samples, S. Van Deusen and M. Harrington for preparing the single-crystal and hot-pressed materials, W. O. Wallace for the Auger analyses, and Karen Higgins for obtaining the Raman spectra.

¹C. Wood and D. Emin, in *Defect Properties and Processing of High-Technology Nonmetallic Materials*, Boston, 1983, Vol. 24 of *Materials Research Society Symposia Proceedings*, edited by J. H. Crawford, Y. Chen, and W. A. Sibley (North-Holland, Amsterdam, 1984), p. 199.

²G. A. Slack, T. F. McNelly, and E. A. Taft, *J. Phys. Chem. Solids* **44**, 1009 (1983).

³B. Morosin, A. W. Mullendore, D. Emin, and G. A. Slack, in *Boron-Rich Solids* (University of New Mexico, Albuquerque, New Mexico), Proceedings of an International Conference on the Physics and Chemistry of Boron and Boron-Rich Borides, AIP Conf. Proc. No. 140, edited by D. Emin, T. L. Aselage, C. L. Beckel, I. A. Howard, and C. Wood (AIP, New York, 1986), pp. 70–86.

⁴M. N. Alexander, in Ref. 3, pp. 168–176.

⁵M. Bouchacourt and F. Thevenot, *J. Less-Common Met.* **82**, 219 (1981).

⁶H. K. Clark and J. L. Hoard, *J. Am. Chem. Soc.* **65**, 2115 (1943).

⁷T. M. Duncan, in Ref. 3, pp. 177–188.

⁸C. Wood and D. Emin, *Phys. Rev. B* **29**, 4582 (1984).

⁹M. Van Schilgaarde and W. A. Harrison, *J. Phys. Chem. Solids* **46**, 1093 (1985).

¹⁰H. L. Yakel, in Ref. 3, pp. 97–108.

¹¹P. J. Bray, in Ref. 3, pp. 142–167.

¹²A. C. Larson, in Ref. 3, pp. 109–113.

¹³A. Kirfel, A. Gupta, and G. Will, *Acta Crystallogr. Sect. B* **35**, 1052 (1979).

¹⁴D. Emin, *Phys. Rev. B* **38**, 6041 (1988).

¹⁵D. Emin, *Phys. Rev. Lett.* **35**, 882 (1975).

- ¹⁶L. J. Azevedo, E. L. Venturini, D. Emin, and C. Wood, *Phys. Rev. B* **32**, 7970 (1985).
- ¹⁷E. L. Venturini, L. J. Azevedo, D. Emin, and C. Wood, in Ref. 3, pp. 292–304.
- ¹⁸E. L. Venturini, D. Emin, and T. L. Aselage, in *Novel Refractory Semiconductors*, Vol. 97 of *Materials Research Society Symposium Proceedings*, edited by D. Emin, T. L. Aselage, and C. Wood, (MRS, Pittsburgh, PA, 1987), pp. 57–62.
- ¹⁹D. Emin, in Ref. 3, pp. 189–205.
- ²⁰C. Wood, D. Emin, and P. E. Gray, *Phys. Rev. B* **31**, 6811 (1985).
- ²¹D. Emin, I. A. Howard, T. A. Green, and C. L. Beckel, in Ref. 18, pp. 83–88.
- ²²A. W. Mullendore, in Ref. 3, p. 42.
- ²³T. L. Aselage, in Ref. 18, pp. 101–111.
- ²⁴D. R. Tallant and K. L. Higgins, in *Proceedings of the Scientific Applications of Lasers Symposium (ICALEO '83)*, Vol. 42 of *Laser Institute of America Proceedings*, edited by R. O. Godwin and J. P. Aldridge (LIA, Toledo, OH, 1983), p. 12.
- ²⁵C. L. Beckel (private communication).
- ²⁶W. Weber and M. F. Thorpe, *J. Phys. Chem. Solids* **36**, 967 (1975).
- ²⁷J. A. Shelnutt, B. Morosin, D. Emin, A. Mullendore, G. Slack, and C. Wood, in Ref. 3, pp. 312–324.
- ²⁸W. Richter, W. Weber, and K. Pflöog, *J. Less-Common Met.* **47**, 85 (1976).
- ²⁹D. Emin, in Ref. 18, pp. 3–15.
- ³⁰B. Morosin (private communication) has carried out x-ray scattering measurements on boron carbide crystals at large diffraction angles. At such angles the difference between the scattering factors for boron and carbon is sufficient to make a determination of the carbon occupancy in the icosahedra from refinements of the x-ray data. His measurements indicate that the carbon atom in $B_{11}C$ icosahedra in boron carbides containing 20 at. % carbon preferentially occupies the polar site (see Fig. 4). For additional evidence of preferential placement of carbon atoms in B_4C polar icosahedral sites, see B. Morosin, A. Mullendore, D. Emin, and G. Slack, in Ref. 3, p. 82, and B. Morosin, T. L. Aselage, and R. S. Feiselson, in Ref. 18, p. 147.
- ³¹M. F. Hawthorne, in *The Chemistry of Boron and its Compounds*, edited by E. L. Muetterties (Wiley, New York, 1967), pp. 304 and 305.